RESEARCH PAPER

Design, Development and Evaluation of Venlafaxine-Loaded Lipid–Polymer Hybrid Nanoparticles for Intranasal Nose-to-Brain Delivery

Mr. Anil Pawar[1*], Dr. Ramesh Ingole[2], Dr. Tejas Pachpute[3]
[1,2,3]Department of Pharmacy, Sabarmati University, Ahmadabad, Gujarat, India
[*]Corresponding Author: Mr. Anil Pawar, Email: anilpawar195@gmail.com
Emails: ramesh.ingole@rediffmail.com, tejaspachpute@gmail.com

ABSTRACT
The present study aimed to develop and optimize venlafaxine-loaded lipid–polymer hybrid nanoparticles (VNF-LPHNPs) for intranasal nose-to-brain delivery. Lipid–polymer hybrid nanoparticles were prepared using hot high-pressure homogenization technique employing glyceryl monostearate (GMS) as lipid, sodium alginate as polymer, Tween 80 as surfactant, and soya lecithin as stabilizer. A 2^3 full factorial design was applied to optimize the effect of lipid concentration, polymer concentration, and surfactant concentration on mean particle size (MPS), zeta potential (ZP), and entrapment efficiency (EE%).
The prepared formulations exhibited particle size in the range of 166–251 nm, zeta potential between −23.1 and −34.7 mV, and entrapment efficiency ranging from 26.4% to 79.9%. Among all formulations, batch F5 showed optimized physicochemical characteristics with particle size of 166 nm, PDI of 0.444, zeta potential of −30.5 mV, and entrapment efficiency of 79.9%. Differential scanning calorimetry (DSC) and X-ray diffraction (XRD) studies confirmed transformation of venlafaxine from crystalline to amorphous form within the lipid–polymer matrix, while Fourier transform infrared spectroscopy (FTIR) analysis demonstrated compatibility between the drug and excipients without significant interaction. Scanning electron microscopy (SEM) and transmission electron microscopy (TEM) revealed formation of stable nanoparticles with uniform morphology and smooth surface characteristics.
Overall, the developed VNF-LPHNPs demonstrated promising physicochemical properties suitable for intranasal drug delivery and may serve as an effective nanoparticulate system for enhanced nose-to-brain delivery of venlafaxine.
Keywords: Venlafaxine hydrochloride, Lipid–polymer hybrid nanoparticles, Intranasal delivery, Nose-to-brain delivery, High-pressure homogenization, Nanoparticles.
How to cite this article: Pawar A, Ingole R, Pachpute T. Design, Development and Evaluation of Venlafaxine-Loaded Lipid–Polymer Hybrid Nanoparticles for Intranasal Nose-to-Brain Delivery. Int J Drug Deliv Technol. 2026;16(51s): 1483-1499. DOI: 10.25258/ijddt.16.51s.110
Source of support: Nil.
Conflict of interest: None

1. Introduction

Depression is a serious and chronic psychiatric disorder that affects millions of individuals globally and significantly reduces quality of life, emotional stability, and social functioning. The growing prevalence of depressive disorders has become a major healthcare concern worldwide, particularly among young and middle-aged populations. Conventional antidepressant therapy mainly relies on oral administration; however, oral delivery often results in poor therapeutic response due to extensive hepatic first-pass metabolism, delayed onset of action, fluctuating plasma drug levels, and limited drug penetration across the blood–brain barrier (BBB) [1–3]. Furthermore, long-term oral administration of antidepressants is associated with systemic adverse effects such as nausea, dizziness, insomnia, hypertension, and gastrointestinal disturbances, which may reduce patient compliance and treatment effectiveness [4,5].

Venlafaxine hydrochloride is a potent serotonin–norepinephrine reuptake inhibitor (SNRI) extensively used for the treatment of major depressive disorder, generalized anxiety disorder, and panic disorders [6]. Although venlafaxine exhibits significant antidepressant activity, its conventional oral delivery suffers from low bioavailability due to extensive first-pass metabolism in the liver, resulting in variable therapeutic outcomes [7]. In addition, only a limited fraction of the administered dose is capable of crossing the blood–brain barrier and

reaching the brain in therapeutically effective concentrations [8,9]. Therefore, the development of an alternative drug delivery system capable of improving brain targeting efficiency and enhancing bioavailability is highly desirable.

In recent years, intranasal drug delivery has emerged as a promising and non-invasive approach for direct nose-to-brain transport of therapeutic agents [10]. The nasal cavity provides a highly vascularized epithelial surface along with direct neuronal connections to the brain through the olfactory and trigeminal pathways [11]. These pathways enable therapeutic agents to bypass the blood–brain barrier and hepatic first-pass metabolism, thereby facilitating rapid and targeted drug delivery to the central nervous system [12]. Intranasal administration also offers several advantages, including rapid onset of action, enhanced bioavailability, reduced systemic exposure, improved patient compliance, and ease of administration [13,14]. Due to these benefits, intranasal drug delivery has gained considerable attention for the treatment of neurological and psychiatric disorders such as depression, Alzheimer's disease, Parkinson's disease, epilepsy, and schizophrenia [15].

Nanotechnology-based drug delivery systems have shown remarkable potential in improving the therapeutic efficacy of drugs intended for brain targeting applications [16]. Various nanosystems such as liposomes, polymeric nanoparticles, nanoemulsions, solid lipid nanoparticles, and nanostructured lipid carriers have been extensively investigated for intranasal delivery of central nervous system drugs [17,18]. Among these, lipid–polymer hybrid nanoparticles (LPHNs) have attracted significant scientific interest because they combine the advantages of both polymeric nanoparticles and lipid-based delivery systems [19]. LPHNs generally consist of a polymeric core surrounded by a lipid shell, providing excellent structural stability, high drug entrapment efficiency, controlled drug release, improved biocompatibility, and enhanced permeation across biological membranes [20,21].

The lipid shell present in LPHNs enhances interaction with the nasal mucosa and facilitates efficient transport across epithelial barriers, whereas the polymeric core provides sustained release characteristics and protects the encapsulated drug from enzymatic degradation [22]. In addition, nanosized hybrid particles exhibit improved mucoadhesion, prolonged nasal residence time, enhanced cellular uptake, and better penetration into brain tissues through olfactory pathways [23,24]. Previous studies have demonstrated that nanoparticle-mediated intranasal drug delivery significantly improves brain bioavailability and therapeutic efficacy compared to conventional formulations [25].

Several recent investigations have reported successful development of intranasal nanoparticulate systems for antidepressant and antipsychotic drugs using polymeric nanoparticles, lipid nanoparticles, nanoemulsions, and hybrid nanocarriers [26]. These nanoformulations exhibited enhanced drug permeation, sustained drug release, improved pharmacokinetic performance, and increased brain uptake efficiency [27]. Moreover, incorporation of bioadhesive and permeation-enhancing materials within nanoparticle systems has further improved nasal retention and direct nose-to-brain transport of therapeutic agents [28]. Such advancements highlight the considerable potential of lipid–polymer hybrid nanoparticles as efficient carriers for targeted antidepressant delivery through the intranasal route [29].

Therefore, the present study was aimed at the design, development, and evaluation of venlafaxine-loaded lipid–polymer hybrid nanoparticles for intranasal nose-to-brain delivery. The developed formulation was

intended to improve brain targeting efficiency, enhance drug bioavailability, provide sustained drug release, and overcome the limitations associated with conventional oral therapy [30]. The prepared nanoparticles were further evaluated for physicochemical characteristics, particle size, polydispersity index, zeta potential, entrapment efficiency, and in vitro drug release behavior to determine their suitability as an effective nanocarrier system for targeted brain delivery of venlafaxine.

2. MATERIALS AND METHODS

2.1 Materials

Venlafaxine hydrochloride was obtained as a gift sample from Mylan Pharma Ltd., Hyderabad, India. Glyceryl monostearate (GMS) was procured from Glenmark Pharmaceuticals Ltd., Mumbai, India. Sodium alginate was obtained from Indoco Remedies Ltd., Navi Mumbai, India. Dextran sulphate and Tween 80 were purchased from HiMedia Laboratories Pvt. Ltd., Mumbai, India. Soya lecithin was obtained from PHOSPHOLIPID GmbH, Germany.

Potassium dihydrogen phosphate (KH_2PO_4) and potassium chloride (KCl) were procured from Qualigens Fine Chemicals, Navi Mumbai, India. Sodium hydroxide (NaOH) was purchased from S.D. Fine Chemicals, Mumbai, India. Methanol and acetonitrile of HPLC grade were obtained from Merck Specialities Pvt. Ltd., Worli, Mumbai, India. Hydrochloric acid (HCl) was procured from Rankem RFCL, Ankleshwar, Gujarat, India. Dichloromethane (DCM) was purchased from HiMedia Laboratories Pvt. Ltd., Mumbai, India. All chemicals and reagents used in the study were of analytical grade and were used without further purification.

2.2 Screening of Lipids

Screening of lipids was performed to identify the most suitable solid lipid for the preparation of venlafaxine-loaded lipid–polymer hybrid nanoparticles (LPHNPs). The solubility of venlafaxine hydrochloride was evaluated in different solid lipids to determine the lipid exhibiting maximum drug solubilization capacity. Selection of an appropriate lipid plays a crucial role in improving drug entrapment efficiency, formulation stability, and drug release characteristics of lipid-based nanoparticulate systems [31].

Briefly, an accurately weighed quantity of venlafaxine hydrochloride (10 mg) was mixed separately with increasing amounts of various molten solid lipids. The mixtures were heated above the melting point of the respective lipids under continuous stirring until a clear and homogeneous mixture was obtained. The lipid–drug mixtures were then allowed to cool gradually to room temperature to facilitate solidification of the lipid matrix. After solidification, the mixtures were visually inspected for the presence of drug crystals or phase separation. The lipid showing maximum drug incorporation without visible crystalline drug precipitation was selected for further formulation development of lipid–polymer hybrid nanoparticles [32].

2.3 Formulation of Venlafaxine-Loaded Lipid–Polymer Hybrid Nanoparticles (VNF-LPHNPs)

Venlafaxine-loaded lipid–polymer hybrid nanoparticles (VNF-LPHNPs) were prepared using a two-step emulsification technique involving high-speed homogenization followed by hot high-pressure homogenization [33,34]. The formulation composition was optimized based on extensive literature review and preliminary trial-and-error experiments. Glyceryl monostearate (GMS) was selected as the solid lipid, sodium alginate as the polymer, Tween 80 as the hydrophilic surfactant, and soya lecithin as the lipophilic co-surfactant.

Initially, the lipid phase was prepared by melting GMS followed by addition of soya lecithin under continuous stirring. The lipidic phase was heated to 80°C until a clear and

homogeneous solution was obtained [35]. Simultaneously, the aqueous phase was prepared by dissolving venlafaxine hydrochloride and dextran sulphate in deionized water at a ratio of 2:1 and allowing the solution to stir at 250 rpm for 2 h to facilitate electrostatic interaction. Tween 80 was separately dissolved in deionized water and mixed with the drug-containing aqueous phase to obtain a single aqueous phase [36].

The hot aqueous phase was then added dropwise into the molten lipid phase with continuous stirring to form a coarse emulsion. Additional deionized water was added to maintain the required volume, and the resulting dispersion was subjected to high-speed homogenization using a high-speed homogenizer (Ultra Turrax Ltd., Mumbai, India) at 13,500 rpm for 4 min to obtain a pre-emulsion [37]. Subsequently, sodium alginate was added to the pre-emulsion and mixed uniformly. The resultant warm pre-emulsion was further processed using a high-pressure homogenizer (PANDA 2K, Niro Soavi, Italy) at an optimized pressure of 1080 bar for seven homogenization cycles to obtain VNF-LPHNP dispersion [38]. The prepared nanoparticles were cooled to room temperature and stored for further characterization studies.

2.4 Optimization of Formulation Variables Using Full Factorial Design

A 2^3 full factorial design was employed for optimization of the formulation variables affecting the characteristics of VNF-LPHNPs [39]. The concentrations of lipid (X_1), polymer (X_2), and surfactant (X_3) were selected as independent variables, whereas mean particle size (Y_1), zeta potential (Y_2), and entrapment efficiency (Y_3) were considered as dependent response variables.

The experimental design and statistical analysis were carried out using Design-Expert® software version 7.0.0. The significance of each model term was evaluated at a confidence level of 95%, where p-values less than 0.05 were considered statistically significant [40]. The experimental data were analyzed using analysis of variance (ANOVA), and various mathematical models including linear, interaction, and quadratic models were evaluated to identify the best-fit model for formulation optimization. Three-dimensional response surface plots and contour plots were generated to study the interaction effects of formulation variables on the measured responses [41].

Table 1: Actual and Coded Values of Independent Variables Used in Full Factorial Design

Independent Variables	Low (-1)	High (+1)
X_1 = Concentration of Lipid (%)	0.5	1.0
X_2 = Concentration of Polymer (%)	0.5	1.0
X_3 = Concentration of Surfactant (%)	0.5	1.0

Table 2: Formulation Composition of VNF-LPHNPs Prepared by 2^3 Full Factorial Design

Run	X_1 (%)	X_2 (%)	X_3 (%)
F1	0.50 (-1)	1.00 (+1)	0.50 (-1)
F2	1.00 (+1)	1.00 (+1)	1.00 (+1)
F3	0.50 (-1)	1.00 (+1)	1.00 (+1)
F4	1.00 (+1)	0.50 (-1)	1.00 (+1)
F5	0.50 (-1)	0.50 (-1)	0.50 (-1)
F6	1.00 (+1)	0.50 (-1)	0.50 (-1)
F7	0.50 (-1)	0.50 (-1)	1.00 (+1)
F8	1.00 (+1)	1.00 (+1)	0.50 (-1)

2.5 Characterization of VNF-LPHNPs

Determination of Mean Particle Size and Polydispersity Index (PDI)

The mean particle size and polydispersity index (PDI) of VNF-LPHNPs were determined using photon correlation spectroscopy (PCS) with a Zetasizer Nano ZS 90 (Malvern Instruments, UK) at 25°C and a scattering angle of 90° [42]. Prior to analysis, the nanoparticle dispersion was diluted appropriately with deionized water to obtain suitable scattering intensity. The average particle diameter and PDI were recorded for all formulations.

Determination of Zeta Potential

Zeta potential measurements were performed using a Zetasizer Nano ZS 90 (Malvern Instruments, UK) at 25°C with an applied electric field of 23 Vm^{-1} [43]. The nanoparticle samples were diluted with deionized water and placed into an electrophoretic cell. The zeta potential values were determined to evaluate the surface charge and physical stability of the prepared nanoparticles.

Determination of Entrapment Efficiency (EE%) and Drug Loading (DL%)

Entrapment efficiency and drug loading of VNF-LPHNPs were determined using ultracentrifugation technique [44]. Briefly, the nanoparticle dispersion was transferred into polyallomer centrifuge tubes and centrifuged using an Optima Max XP ultracentrifuge (Beckman Coulter, USA) at 50,000 rpm for 30 min at 4°C. The amount of unentrapped venlafaxine present in the supernatant was analyzed using a UV–Visible spectrophotometer (UV-1700, Shimadzu, Japan) at 240 nm.

Lyophilization of VNF-LPHNPs

The optimized VNF-LPHNP formulation was subjected to lyophilization to improve long-term stability and storage characteristics [45]. The nanoparticle dispersion was frozen and subsequently freeze-dried under controlled conditions to obtain dry nanoparticulate powder suitable for further characterization.

Percentage Yield

Percentage yield of VNF-LPHNPs was calculated based on the ratio of the weight of recovered nanoparticles to the total weight of drug and excipients used during formulation preparation [46].

Differential Scanning Calorimetry (DSC) Studies

Thermal characterization of VNF-LPHNPs was carried out using differential scanning calorimetry (DSC 1 STARe System, Mettler-Toledo, Switzerland) [47]. The samples were analyzed at a heating rate of 10°C/min over a temperature range of 40–400°C under nitrogen purge atmosphere. DSC studies were performed for pure venlafaxine hydrochloride (VNF), bulk GMS, physical mixture of VNF and GMS (1:1 ratio), and freeze-dried optimized VNF-LPHNPs.

X-Ray Diffraction (XRD)

The crystalline characteristics of VNF and optimized VNF-LPHNPs were evaluated using an X-ray diffractometer (Bruker AXS D8 Advance, Germany) [48]. The samples were mounted on the sample holder and scanned over a diffraction angle range of 5–90° at a scanning speed of 5°/min. The samples analyzed included pure VNF, physical mixture (1:1 ratio), and lyophilized optimized VNF-LPHNP formulation.

Fourier Transform Infrared Spectroscopy (FTIR)

FTIR analysis of VNF-LPHNPs was performed using a Fourier Transform Infrared spectrophotometer (Shimadzu 8400S, Japan) [49]. The samples were mixed with IR-grade potassium bromide (KBr) in a ratio of 1:100 and compressed into pellets using a motorized pellet press (Kimaya Engineers, India) at a pressure of 10–12 tons. The prepared pellets were scanned to evaluate possible interactions between the drug and formulation excipients.'

Scanning Electron Microscopy (SEM)

Surface morphology of the lyophilized VNF-LPHNPs was analyzed using scanning electron microscopy (JEOL 6390LV, STIC, Cochin). The samples were mounted on double-sided carbon tape, gold coated using ion sputtering for 10 min, and observed under SEM at an operating voltage of 20 kV at different magnifications [50].

Transmission Electron Microscopy (TEM)

Transmission electron microscopy was used to evaluate the morphology of VNF-LPHNPs. The nanoparticle dispersion was negatively stained with phosphotungstic acid (PTA), and a drop of diluted sample was placed on copper grids. Excess liquid was removed after 3 min, and the grids were air dried before imaging using TEM (STIC, Cochin) [51].

3. Result and Discussion

3.1 Screening of Lipids

Selection of a suitable solid lipid is an important criterion in the development of lipid–polymer hybrid nanoparticles, as it significantly influences drug solubility, entrapment efficiency, particle stability, and release characteristics of the formulation. In the present study, the solubility of venlafaxine hydrochloride (VNF) was evaluated in different solid lipids including lauric acid, stearic acid, palmitic acid, Precirol, and glyceryl monostearate (GMS). The obtained results are presented in Table 3. Among the investigated lipids, GMS exhibited the highest solubilization capacity for venlafaxine with a drug-to-lipid ratio of 1:06, whereas Precirol, stearic acid, lauric acid, and palmitic acid showed comparatively lower solubility of the drug. The higher solubility of venlafaxine in GMS may be attributed to its better lipid matrix compatibility and enhanced drug incorporation ability. Improved drug solubilization within the lipid phase is advantageous for achieving higher entrapment efficiency and formulation stability in nanoparticulate systems.

Furthermore, all formulations prepared using GMS exhibited desirable particle size and good physical stability, indicating its suitability for the preparation of VNF-LPHNPs. In addition, GMS is biocompatible, non-toxic, economically feasible, and categorized under Generally Recognized as Safe (GRAS) excipients, making it an appropriate lipid candidate for intranasal pharmaceutical formulations. Based on these findings, GMS was selected as the optimized solid lipid for further formulation and characterization studies of venlafaxine-loaded lipid–polymer hybrid nanoparticles.

Table 3: Solubility of Venlafaxine in Different Solid Lipids

Sr. No.	Solid Lipids	Solubility of drug (mg/gm)
1	Lauric acid	1:12
2	Stearic acid	1:15
3	Palmitic acid	1:12
4	Precirol	1:17
5	GMS	1:06

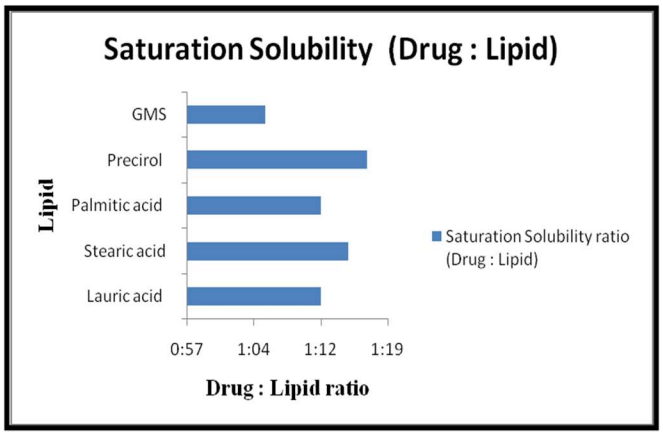

Figure 1: Solubility of VNF in different Solid Lipid

3.2 Development and Optimization of VNF-Loaded LPHNPs

Venlafaxine-loaded lipid–polymer hybrid nanoparticles (VNF-LPHNPs) were

successfully prepared using hot high-pressure homogenization technique. The formulation composition and processing conditions were optimized based on preliminary trials and extensive literature survey. Glyceryl monostearate (GMS) was selected as the solid lipid, sodium alginate as the polymeric stabilizer, Tween 80 as the hydrophilic surfactant, and soya lecithin as the lipophilic co-surfactant for the preparation of stable nanoparticulate formulations.

Initially, GMS and soya lecithin were melted together to form a clear lipidic phase at 80°C. Simultaneously, the aqueous phase containing venlafaxine hydrochloride and dextran sulphate in a ratio of 2:1 was prepared and subjected to mild stirring for 2 h to facilitate electrostatic interaction between the components. Tween 80 solution was then mixed with the drug-containing aqueous phase and heated to the same temperature as the lipid phase. The hot aqueous phase was gradually dispersed into the molten lipid phase under continuous stirring to obtain a milky white coarse emulsion. Further homogenization at 13,500 rpm for 4 min resulted in formation of a stable pre-emulsion. Sodium alginate was subsequently added to the pre-emulsion and mixed thoroughly before subjecting the system to high-pressure homogenization at 1080 bar for seven cycles to obtain VNF-LPHNP dispersion.

The prepared formulations exhibited good physical appearance and formed stable nanoparticulate dispersions without visible aggregation or phase separation. The use of high-pressure homogenization technique was found to be highly effective for the preparation of lipid–polymer hybrid nanoparticles due to its reproducibility, scalability, and ability to produce nanoparticles within the nanometric range. The optimized homogenization pressure and cycle number significantly influenced particle size and stability of the developed formulation.

It was observed from preliminary optimization studies that increasing homogenization cycles beyond seven resulted in particle aggregation and slight increase in particle size, possibly due to enhanced kinetic collision among nanoparticles. Therefore, seven homogenization cycles were considered optimum for the preparation of stable nanoparticles with desirable particle size distribution. Furthermore, the combination of sodium alginate and soya lecithin contributed to improved stabilization of nanoparticles and enhanced storage stability compared to systems containing a single surfactant or stabilizer.

The developed VNF-LPHNPs were found to possess desirable physicochemical properties suitable for intranasal drug delivery applications. The optimized formulation strategy was further evaluated using factorial design to study the influence of formulation variables on particle size, zeta potential, and entrapment efficiency of the nanoparticles.

3.3 Optimization and Validation of VNF-LPHNPs

A 2^3 full factorial design was employed to optimize the formulation variables affecting the characteristics of VNF-LPHNPs. The effect of lipid concentration (X_1), polymer concentration (X_2), and surfactant concentration (X_3) on mean particle size (MPS), zeta potential (ZP), entrapment efficiency (EE%), and drug loading (DL%) was evaluated. The characterization results of all prepared formulations are presented in Table 4.

The mean particle size of the developed formulations ranged from 166 ± 0.42 to 251 ± 0.11 nm, indicating successful preparation of nanoparticles within the desired nanometric range. Formulation F5 exhibited the lowest particle size, whereas F7 showed the highest particle size. The zeta potential

values ranged from −23.1 ± 0.24 to −34.7 ± 0.32 mV, confirming good physical stability of the prepared nanoparticles. Entrapment efficiency was observed in the range of 26.4 ± 0.26% to 83.5 ± 0.15%, while drug loading ranged from 11.56 ± 0.46% to 17.19 ± 0.68%. Among all formulations, batch F5 demonstrated desirable physicochemical characteristics with smaller particle size, low PDI, higher entrapment efficiency, and better drug loading, and was therefore selected as the optimized formulation for further studies.

Table 4: 2^3 Full factorial design parameters, formulation composition and characterization of VNF-LPHNPs

Run	Factors			Responses				
	X_1 (%)	X_2 (%)	X_3 (%)	MPS Y_1 (nm)	ZP Y_2	PDI	EE Y_3 (%)	DL (%)
F1	0.50(-1)	1.00(+1)	0.50(-1)	200 ± 0.21	-34.7 ± 0.32	0.611 ± 0.05	74.7 ± 0.46	15.87 ± 0.17
F2	1.00(+1)	1.00(+1)	1.00(+1)	170 ± 0.53	-23.1 ± 0.24	0.461 ± 0.03	26.4 ± 0.26	13.19 ± 0.37
F3	0.50(-1)	1.00(+1)	1.00(+1)	246 ± 0.77	-32.8 ± 0.14	0.809 ± 0.009	52.5 ± 0.66	11.56 ± 0.46
F4	1.00(+1)	0.50(-1)	1.00(+1)	169 ± 0.34	-22.1 ± 0.48	0.462 ± 0.006	61.8 ± 0.51	12.75 ± 0.27
F5	**0.50(-1)**	**0.50(-1)**	**0.50(-1)**	**166 ± 0.42**	**-30.5 ± 0.52**	**0.444 ± 0.002**	**79.9 ± 0.91**	**17.19 ± 0.68**
F6	1.00(+1)	0.50(-1)	0.50(-1)	187 ± 0.75	-26.6 ± 0.37	0.537 ± 0.008	34.5 ± 0.34	14.67 ± 0.73
F7	0.50(-1)	0.50(-1)	1.00(+1)	251 ± 0.11	-27.6 ± 0.65	0.582 ± 0.016	83.5 ± 0.15	12.22 ± 0.55

F 8	1.0 0(+ 1)	1.0 0(+ 1)	0.5 0(- 1)	1 7 0 ± 0. 2 2	- 3 3. 4 ± 0. 5 5	0. 5 4 1 ± 0. 0 9	2 7. 2 ± 0. 6 2	1 3. 1 4 ± 4 1

Independent variables: X_1 = Lipid concentration, X_2 = Polymer concentration, X_3 = Surfactant concentration. variables: Y_1 = Mean particle size (MPS), Y_2 = Zeta potential (ZP), Y_3 = Entrapment efficiency (EE%). Values are expressed as mean ± SD (n = 3).

3.4 Optimization Data Analysis and Model Validation

The responses obtained for mean particle size (Y_1), zeta potential (Y_2), and entrapment efficiency (Y_3) were analyzed using Design Expert® software (Version 7.0.0, State-Ease Inc., Minneapolis, USA). The observed values for particle size, zeta potential, and entrapment efficiency ranged from 166 ± 0.42 to 251 ± 0.11 nm, −23.1 ± 0.24 to −34.7 ± 0.32 mV, and 26.4 ± 0.26% to 79.9 ± 0.91%, respectively.All experimental responses obtained from the eight formulations were fitted into various statistical models, and the main effect model was found to be the best fit for particle size, zeta potential, and entrapment efficiency. The ANOVA results demonstrated that the selected model was statistically significant for all three response variables, with p-values less than 0.05.

Table 5: ANOVA Analysis of Response Variables

Parameters	SS	DF	MS	*F*-Value	*P* Value	Model Significance
1.MPS (nm)						
Model	7857.38	3	2619.13	14.24	0.0133	**Significant**
2. ZP						
Model	137.02	3	45.67	8.51	0.0328	**Significant**
3. EE (%)						
Model	3260.51	3	1086.84	6.97	0.0456	**Significant**

SS = Sum of squares; DF = Degrees of freedom; MS = Mean square. P-values less than 0.05 were considered statistically significant.

3.5 Response Surface Plot Analysis

Three-dimensional response surface plots generated using Design-Expert® software were used to study the interaction effects of lipid concentration, polymer concentration, and surfactant concentration on mean particle size, zeta potential, and entrapment efficiency of VNF-LPHNPs.

The response surface plots for mean particle size demonstrated that increasing lipid concentration resulted in reduction of particle size, whereas higher surfactant concentration slightly increased the particle size. However, simultaneous interaction between lipid and surfactant concentration produced comparatively smaller nanoparticles, indicating significant influence of formulation variables on particle size distribution. The response surface plots for zeta potential showed that increasing lipid and surfactant concentration increased the zeta potential values, while increasing polymer concentration resulted in reduction of zeta potential. The obtained zeta potential values confirmed good stability of the developed nanoparticulate formulations.

Similarly, the response surface plots for entrapment efficiency indicated that increasing surfactant concentration improved drug entrapment, whereas excessive lipid and polymer concentration reduced the entrapment efficiency. This may be attributed to lipid precipitation during nanoparticle formation, leading to incomplete drug encapsulation and partitioning of drug into the external aqueous phase. Overall, the response surface analysis confirmed that lipid concentration, polymer concentration, and surfactant concentration significantly affected the physicochemical characteristics of VNF-LPHNPs and played an important role in optimization of the formulation.

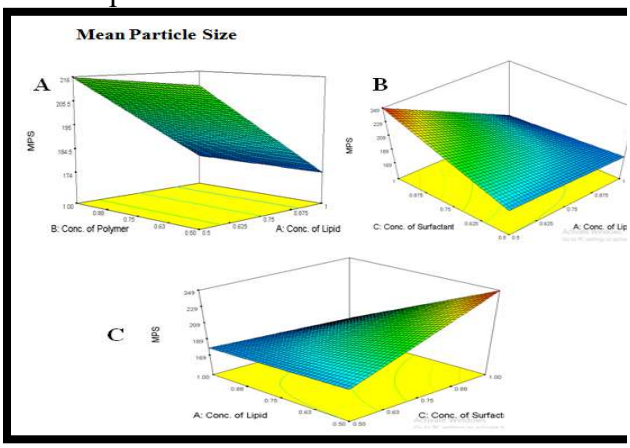

Figure 2: Response surface plots showing the effect of lipid concentration, polymer concentration, and surfactant concentration on mean particle size of VNF-LPHNPs.

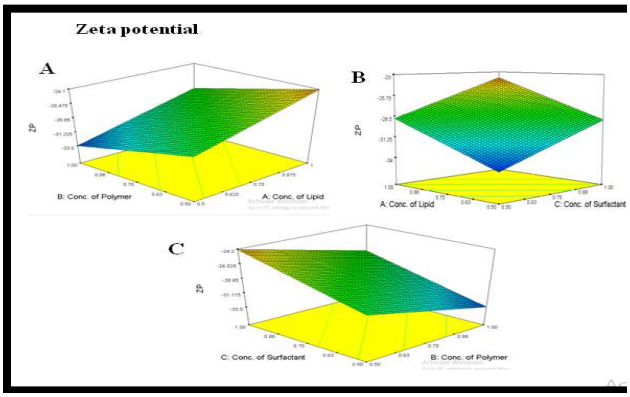

Figure 3: Response surface plots showing the effect of lipid concentration, polymer concentration, and surfactant concentration on zeta potential of VNF-LPHNPs.

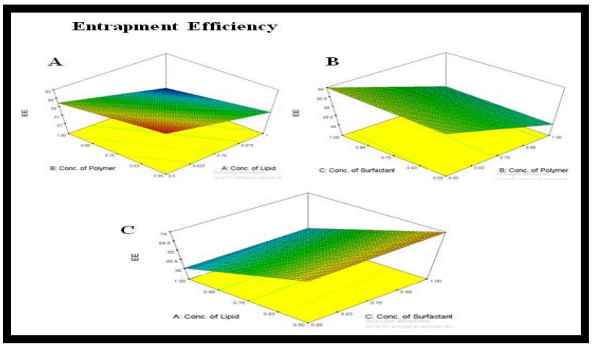

Figure 4: Response surface plots showing the effect of lipid concentration, polymer concentration, and surfactant concentration on entrapment efficiency of VNF-LPHNPs.

3.6 Characterization of VNF-LPHNPs

Particle Size

The particle size and polydispersity index (PDI) of the developed VNF-LPHNP formulations were observed in the range of 166–251 nm and 0.444–0.809, respectively. The optimized formulation (F5) exhibited a mean particle size of 166 nm with a PDI value of 0.444, indicating narrow particle size distribution and good homogeneity of the nanoparticulate system. The obtained particle size was considered suitable for intranasal delivery and efficient uptake of nanoparticles.

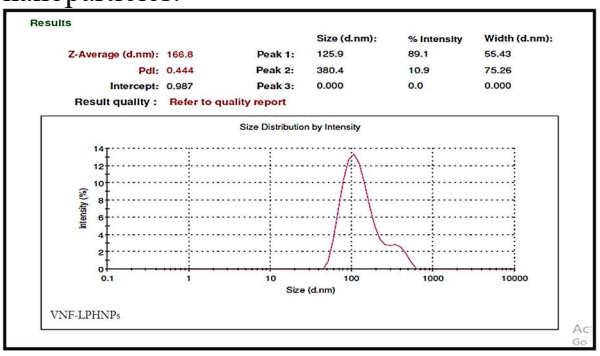

Figure 5: Particle size and polydispersity index (PDI) of optimized VNF-LPHNP formulation.

Zeta Potential

The zeta potential of the optimized VNF-LPHNP formulation was found to be −30.5 mV, indicating good physical stability of the

nanoparticulate system. The negative surface charge was mainly attributed to the presence of negatively charged GMS, sodium alginate, and Tween 80 in the formulation. The zeta potential values of all formulations ranged from −23.1 to −34.7 mV, suggesting sufficient electrostatic repulsion between nanoparticles and reduced tendency for aggregation.

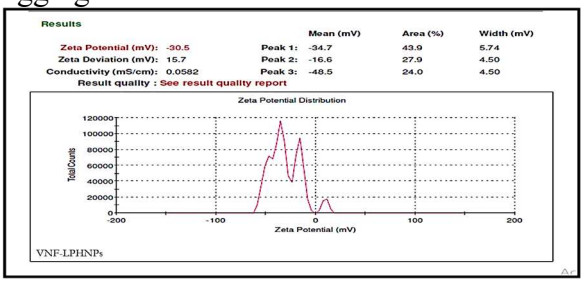

Figure 6: Zeta potential of optimized VNF-LPHNP formulation.

Entrapment Efficiency (EE%) and Drug Loading (DL%)

Venlafaxine-loaded lipid–polymer hybrid nanoparticles (VNF-LPHNPs) were successfully prepared using different lipid concentrations while maintaining a constant drug concentration throughout the formulation process. The entrapment efficiency and drug loading values of all formulations were found to range from 26.4% to 79.9% and 12.75% to 17.19%, respectively.

The optimized formulation exhibited comparatively higher entrapment efficiency and drug loading, which may be attributed to the higher solubility of venlafaxine in glyceryl monostearate (GMS) and efficient incorporation of the drug within the lipid–polymer matrix. The obtained results indicated successful encapsulation of venlafaxine within the developed nanoparticulate system.

Differential Scanning Calorimetry (DSC)

Differential scanning calorimetry (DSC) analysis was performed to evaluate the thermal behavior and compatibility of venlafaxine hydrochloride (VNF) with formulation excipients. The DSC thermograms of pure VNF, GMS, sodium alginate, physical mixture, and freeze-dried optimized VNF-LPHNPs are shown in Figure 7. The DSC thermogram of pure VNF showed a sharp endothermic peak at 227.99°C corresponding to its crystalline nature, while GMS exhibited an endothermic peak at 56.11°C. Sodium alginate showed a characteristic peak at 217.27°C. In the physical mixture, the characteristic peaks of VNF and GMS were retained without significant shifting, indicating absence of chemical interaction between the drug and excipients.

In the DSC thermogram of freeze-dried optimized VNF-LPHNPs, the characteristic endothermic peak of VNF disappeared, whereas broad endothermic peaks corresponding to GMS and mannitol were observed at 41.11°C and around 173°C, respectively. The disappearance of the drug peak suggested molecular dispersion of VNF within the lipid–polymer matrix and transformation of the drug from crystalline to amorphous form during high-pressure homogenization. The obtained results confirmed successful incorporation of VNF into the lipid–polymer hybrid nanoparticulate system without any significant drug–excipient interaction. The amorphous nature of the encapsulated drug may further contribute to improved solubility and enhanced drug release characteristics of the developed formulation.

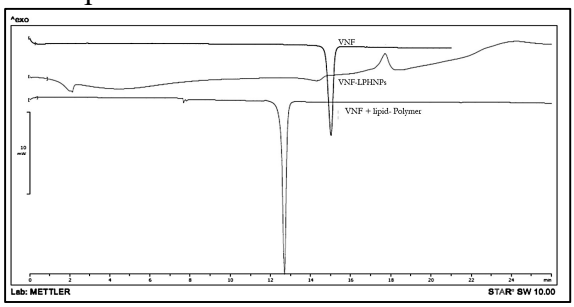

Figure 7: DSC thermograms of pure VNF (A), GMS (B), physical mixture (C), and freeze-dried optimized VNF-LPHNPs (D).

X-Ray Diffraction (XRD)

The X-ray diffraction patterns of pure VNF, physical mixture of VNF with GMS and sodium alginate, and freeze-dried optimized VNF-LPHNPs are shown in Figures 8–11.

The XRD pattern of pure VNF exhibited characteristic sharp diffraction peaks at 2θ values of 8.36°, 8.41°, 11.97°, 13.14°, 14.99°, 17.53°, 17.58°, 17.63°, 18.41°, 20.01°, 23.28°, 24.11°, 24.99°, and 28.16°, confirming the crystalline nature of the drug. The physical mixture showed reduced intensity of characteristic peaks of VNF along with GMS and sodium alginate, indicating partial reduction in crystallinity.In contrast, the freeze-dried VNF-LPHNPs did not exhibit the characteristic sharp peaks of VNF, suggesting conversion of the drug from crystalline to amorphous form or molecular dispersion within the lipid–polymer matrix. The absence of significant changes in diffraction patterns further confirmed compatibility between VNF and formulation excipients without any major physicochemical interaction.

The obtained XRD results indicated successful incorporation of VNF into the lipid–polymer hybrid nanoparticles and transformation of the drug into an amorphous state, which may contribute to improved solubility and enhanced drug release behavior.

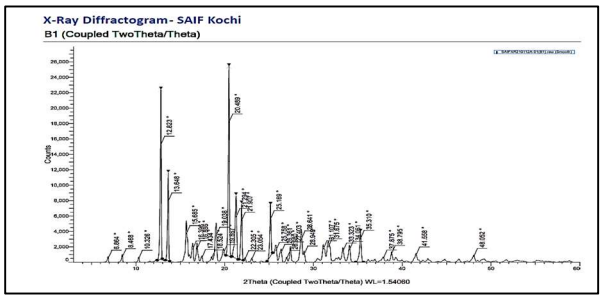

Figure 8: X-ray diffractogram of pure VNF.

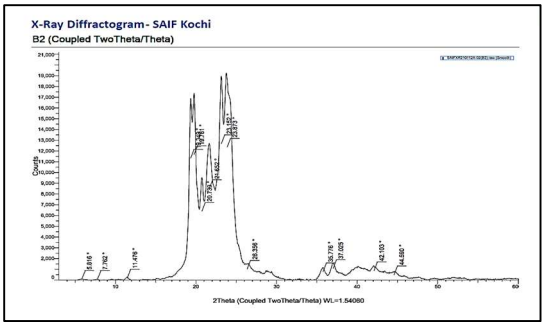

Figure 9: X-ray diffraction pattern of physical mixture.

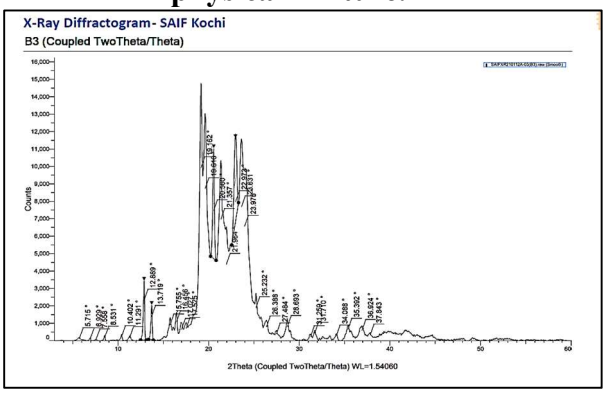

Figure 10: X-ray diffraction pattern of freeze-dried optimized VNF-LPHNPs.

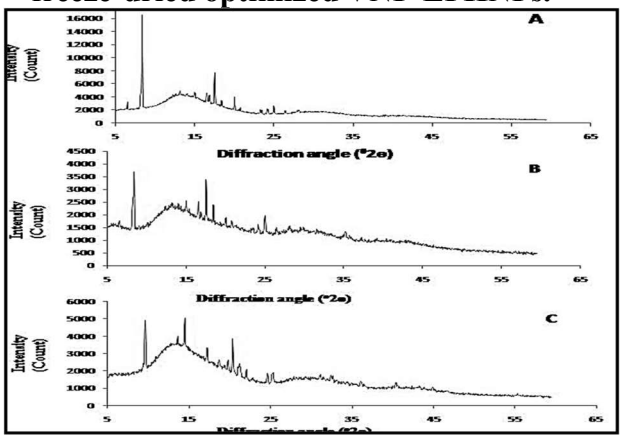

Figure 11: Overlay XRD pattern of pure VNF, physical mixture, and freeze-dried VNF-LPHNPs.

Fourier Transform Infrared Spectroscopy (FTIR)

FTIR spectroscopy was performed to evaluate possible interactions between venlafaxine hydrochloride (VNF) and formulation excipients in the developed VNF-LPHNPs. The FTIR spectra of pure VNF, GMS, sodium alginate, physical mixture, blank LPHNPs, and freeze-dried

optimized VNF-LPHNPs were analyzed and compared.The FTIR spectrum of VNF-LPHNPs showed the characteristic peaks of VNF along with lipid and polymer components without any significant shifting or disappearance of major peaks. The spectra of drug-loaded VNF-LPHNPs were found to be comparable with those of the blank LPHNPs, indicating absence of significant chemical interaction between the drug and excipients.The obtained results confirmed successful incorporation of VNF into the lipid–polymer matrix without affecting the chemical stability of the drug. The absence of major changes in the FTIR spectra suggested compatibility of VNF with GMS and sodium alginate, indicating formation of a stable nanoparticulate formulation.

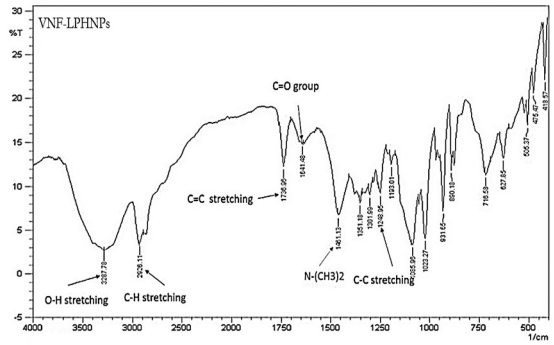

Figure 12: FTIR spectra of freeze-dried optimized VNF-LPHNPs.

Scanning Electron Microscopy (SEM)

The surface morphology of the optimized VNF-LPHNP formulation was evaluated using scanning electron microscopy (SEM). The SEM micrograph revealed formation of dense and rough-surfaced nanoparticles with uniform distribution, as shown in Figure 13. The dense and cross-linked structure of the nanoparticles suggested the presence of a compact polymeric matrix, which may contribute to controlled drug release behavior of the formulation.

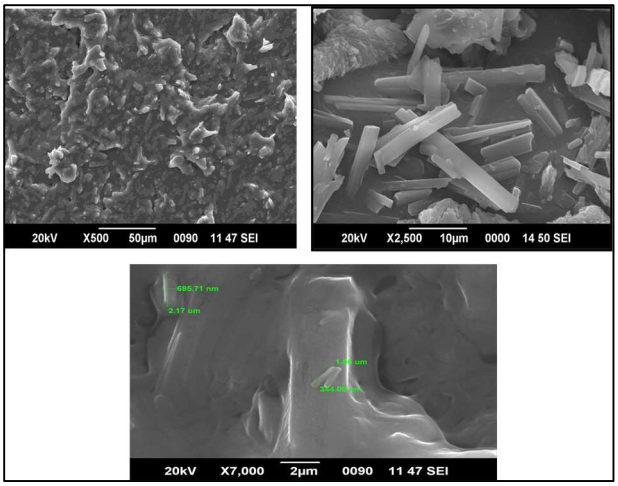

Figure 13: Scanning electron micrograph of optimized VNF-LPHNPs.

Transmission Electron Microscopy (TEM)

Transmission electron microscopy (TEM) analysis was performed to further evaluate the morphology of the optimized VNF-LPHNP formulation. The TEM image confirmed the formation of well-defined spherical nanoparticles with smooth surface morphology, as presented in Figure 14. The presence of a lipid coat surrounding the polymeric core was also observed, confirming successful formation of lipid–polymer hybrid nanoparticles. No visible drug crystals were detected, indicating uniform distribution of venlafaxine within the nanoparticulate system.

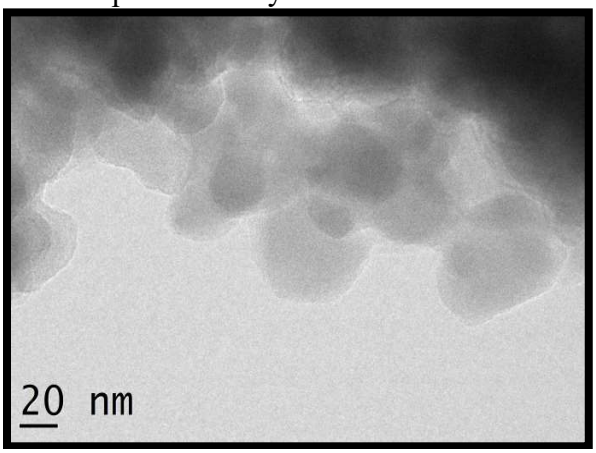

Figure 14: Transmission electron micrograph of optimized VNF-LPHNPs.

Conclusion

In the present study, venlafaxine-loaded lipid–polymer hybrid nanoparticles (VNF-LPHNPs) were successfully developed and optimized for intranasal nose-to-brain delivery. Glyceryl monostearate (GMS) was selected as the optimized solid lipid based on its superior drug solubilization capacity and compatibility with formulation components. The prepared VNF-LPHNPs exhibited desirable physicochemical characteristics including nanosized particle distribution, suitable zeta potential, satisfactory entrapment efficiency, and good drug loading capacity.

Optimization using a 2^3 full factorial design demonstrated significant influence of lipid, polymer, and surfactant concentrations on particle size, zeta potential, and entrapment efficiency of the developed nanoparticles. The optimized formulation showed uniform particle distribution with good physical stability and successful incorporation of venlafaxine within the lipid–polymer matrix. DSC and XRD studies confirmed transformation of venlafaxine from crystalline to amorphous form, while FTIR analysis demonstrated compatibility between the drug and formulation excipients without significant interaction. SEM and TEM studies further confirmed successful formation of lipid–polymer hybrid nanoparticles with uniform morphology and smooth surface characteristics.

Overall, the developed VNF-LPHNPs demonstrated promising physicochemical properties suitable for intranasal drug delivery applications and may serve as an effective nanoparticulate system for enhanced nose-to-brain delivery of venlafaxine.

Abbreviations

BBB–Blood–Brain Barrier, CNS–Central Nervous System, DSC–Differential Scanning Calorimetry, DL–Drug Loading, EE–Entrapment Efficiency, FTIR–Fourier Transform Infrared Spectroscopy, GMS–Glyceryl Monostearate, HPH–High Pressure Homogenization, LPHNPs–Lipid–Polymer Hybrid Nanoparticles, MPS–Mean Particle Size, PBS–Phosphate Buffer Saline, PCS–Photon Correlation Spectroscopy, PDI–Polydispersity Index, SEM–Scanning Electron Microscopy, TEM–Transmission Electron Microscopy, VNF–Venlafaxine Hydrochloride, XRD–X-Ray Diffraction, ZP–Zeta Potential.

Acknowledgement

The authors are thankful to the Department of Pharmacy, Sabarmati University (SU), Ahmedabad, Gujarat, India, for providing the necessary facilities and support to carry out the present research work. The authors also express sincere gratitude to all faculty members and laboratory staff for their valuable guidance and cooperation during the study.

Conflict of Interest

The authors declare that there is no conflict of interest regarding the publication of this manuscript.

Funding

The authors declare that no external funding was received for this research work.

Artificial Intelligence (AI) Statement

The authors confirm that artificial intelligence (AI)-assisted tools were used only for language refinement and grammatical improvement during manuscript preparation. All scientific content, experimental work, data analysis, interpretation, and conclusions were performed and verified by the authors.

Refrences

1. Alberto M, Paiva-Santos AC, Veiga F, Pires PC. Lipid and Polymeric Nanoparticles for Nose-to-Brain Delivery in Depression Therapy. Pharmaceutics. 2022;14(12):2742.
2. Upadhyay R, Ghosh P, Desavathu M. Advances in Nose-to-Brain Drug Delivery of Antidepressants.

International Journal of Pharmaceutics. 2024;648:124866.
3. Nguyen LTT, Duong VA. Nose-to-Brain Drug Delivery: Current Perspectives. Encyclopedia. 2025;5(3):91.
4. Bains N, et al. Current Challenges in Antidepressant Drug Therapy. Journal of Psychiatric Research. 2023;158:45–58.
5. Kaur H, et al. Oral Antidepressant Therapy and Systemic Adverse Effects. Current Drug Therapy. 2022;17(4):255–266.
6. Sharma A, et al. Venlafaxine Hydrochloride: Pharmacological and Clinical Applications. Drug Development Research. 2022;83(5):1098–1110.
7. Patel D, et al. Bioavailability Challenges Associated with Venlafaxine Delivery. Pharmaceutical Sciences Review. 2023;12(2):87–95.
8. Lee D, Minko T. Nanotherapeutics for Nose-to-Brain Drug Delivery. Pharmaceutics. 2022;14(1):42.
9. Crowe TP, et al. Barriers in Brain Drug Delivery and Nasal Transport. Pharmaceutics. 2022;14(3):567.
10. Bahadur S, et al. Intranasal Nanoemulsion Systems for Brain Delivery. Pharmaceutics. 2023;15(2):611.
11. Lochhead JJ, et al. Mechanisms of Intranasal Brain Delivery. Life Sciences. 2022;305:120749.
12. Upadhyay R, et al. Direct Nose-to-Brain Delivery of CNS Therapeutics. International Journal of Pharmaceutics. 2024;648:124866.
13. Nguyen LTT, et al. Intranasal Administration and Brain Targeting. Encyclopedia. 2025;5(3):91.
14. Alsaad AA, et al. Intranasal Nanocarriers for CNS Disorders. Drug Delivery and Translational Research. 2022;12:1142–1160.
15. Ahmed RZ, et al. Nasal In Situ Gel Systems for Brain Delivery. World Journal of Pharmaceutical Research. 2022;11(8):1120–1138.
16. Pinto M, et al. Nanoparticles as Brain Drug Delivery Platforms. Ageing Research Reviews. 2022;75:101574.
17. Kumbhar SA, et al. Mucoadhesive Nanoemulsions for Intranasal Brain Targeting. International Journal of Pharmaceutics. 2022;627:122207.
18. Abourehab MA, et al. Nanostructured Lipid Carriers and Brain Delivery Applications. Journal of Materials Chemistry B. 2022;10(25):4789–4807.
19. Aibani N, et al. Lipid–Polymer Hybrid Nanoparticles for Drug Delivery Applications. Pharmaceutics. 2022;14(9):1834.
20. Alghareeb S, et al. PLGA Hybrid Nanoparticles for Nasal Drug Delivery. Journal of Drug Delivery Science and Technology. 2024;91:105270.
21. Kaur J, et al. Advances in Hybrid Nanocarrier Systems for CNS Disorders. Chemical Biology Interactions. 2022;365:110091.
22. Seju U, et al. Polymeric Nanoparticles for Nose-to-Brain Delivery. Acta Biomaterialia. 2022;147:192–209.
23. Sawant K, et al. Polycaprolactone Nanoparticles for Brain Delivery Applications. Materials Science and Engineering C. 2022;134:112690.
24. Amkar AJ, et al. Nanogel-Based Systems for Intranasal Brain Delivery. Engineering Proceedings. 2023;37(1):15.
25. Piazza J, et al. PEG-PLGA Nanoparticles for Enhanced Brain Uptake. European Journal of

Pharmaceutics and Biopharmaceutics. 2022;174:23–35.
26. Ali ZH, et al. Nanoemulsion-Based Intranasal Systems for Antidepressant Delivery. Journal of Excipients and Food Chemistry. 2023;14(2):78–92.
27. Khute S, et al. Optimization of Venlafaxine Nasal Liposome Formulation. Pharmaceutics. 2023;15(4):1215.
28. Patel HP, et al. Bioadhesive Nanocarriers for Nose-to-Brain Drug Delivery. Journal of Drug Delivery Science and Technology. 2022;74:103556.
29. Alberto M, et al. Hybrid Nanoparticle Systems for CNS Drug Targeting. Pharmaceutics. 2022;14(12):2742.
30. Xinchen Y, et al. Lipid-Based Nanoparticles via Nose-to-Brain Delivery. Frontiers in Cell and Developmental Biology. 2023;11:1214450.
31. Aibani N, et al. Lipid–Polymer Hybrid Nanoparticles for Drug Delivery Applications. Pharmaceutics. 2022;14(9):1834.
32. Abourehab MA, et al. Nanostructured Lipid Carriers and Hybrid Lipid Systems for Drug Delivery Applications. Journal of Materials Chemistry B. 2022;10(25):4789–4807.
33. Aibani N, et al. Lipid–Polymer Hybrid Nanoparticles for Drug Delivery Applications. Pharmaceutics. 2022;14(9):1834.
34. Upadhyay R, et al. Hybrid Nanocarriers for Nose-to-Brain Drug Delivery. International Journal of Pharmaceutics. 2024;648:124866.
35. Abourehab MA, et al. Lipid-Based Nanocarriers for CNS Delivery. Journal of Materials Chemistry B. 2022;10(25):4789–4807.
36. Alberto M, et al. Polymeric and Lipid Nanoparticles for Brain Delivery. Pharmaceutics. 2022;14(12):2742.
37. Kaur J, et al. High-Speed Homogenization Techniques in Nanoparticle Development. Chemical Biology Interactions. 2022;365:110091.
38. Pinto M, et al. High-Pressure Homogenization for Nanoparticle Formulation. Ageing Research Reviews. 2022;75:101574.
39. Patel HP, et al. Statistical Optimization of Nanoparticulate Systems. Journal of Drug Delivery Science and Technology. 2022;74:103556.
40. Sawant K, et al. Design Expert-Based Optimization of Polymeric Nanoparticles. Materials Science and Engineering C. 2022;134:112690.
41. Amkar AJ, et al. Factorial Design Optimization in Nanogel Systems. Engineering Proceedings. 2023;37(1):15.
42. Seju U, et al. Particle Size Analysis of Nanoparticulate Systems. Acta Biomaterialia. 2022;147:192–209.
43. Lochhead JJ, et al. Surface Charge Characterization of Nanocarriers. Life Sciences. 2022;305:120749.
44. Khute S, et al. Entrapment Efficiency Evaluation of Venlafaxine Nanocarriers. Pharmaceutics. 2023;15(4):1215.
45. Alghareeb S, et al. Freeze Drying of Hybrid Nanoparticles. Journal of Drug Delivery Science and Technology. 2024;91:105270.
46. Ahmed RZ, et al. Evaluation Parameters of Nanoparticles for Brain Delivery. World Journal of Pharmaceutical Research. 2022;11(8):1120–1138.
47. Bahadur S, et al. In Vitro Release Studies of Intranasal

Nanoformulations. Pharmaceutics. 2023;15(2):611.
48. Piazza J, et al. Dialysis Membrane-Based Drug Release Studies. European Journal of Pharmaceutics and Biopharmaceutics. 2022;174:23–35.
49. Ali ZH, et al. UV Spectrophotometric Evaluation of Nanoemulsion Systems. Journal of Excipients and Food Chemistry. 2023;14(2):78–92.
50. Lee D, Minko T. Drug Release Kinetics and Mechanisms in Nanotherapeutics. Pharmaceutics. 2022;14(1):42.